

Band structure of the Ca/Si(111)-(2×1) surfaceKazuyuki Sakamoto,^{1,*} H. M. Zhang,² and R. I. G. Uhrberg²¹*Department of Physics, Graduate School of Science, Tohoku University, Sendai 980-8578, Japan*²*Department of Physics and Measurement Technology, Linköping University, S-581 83 Linköping, Sweden*

(Received 13 August 2003; published 22 December 2003)

We have investigated the electronic structure of the Ca/Si(111)-(2×1) surface using angle-resolved photoelectron spectroscopy. Two semiconducting surface states were clearly observed in the bulk band gap, and one was found in a pocket of the bulk band projection. Qualitatively, the dispersions of the two surface states observed in the band gap agree well with theoretical dispersions for a clean Si(111)-(2×1) surface with the Seiwatz structure. Taking this result into account, we conclude that the two surface states in the band gap originate from orbitals of Si atoms that form a Seiwatz structure, and that two electrons are donated from Ca to Si per (2×1) unit cell. This conclusion supports the structure of the Ca/Si(111)-(2×1) surface proposed in the literature.

DOI: 10.1103/PhysRevB.68.245316

PACS number(s): 73.20.At, 79.60.-i, 61.14.Hg

I. INTRODUCTION

In the past decade, one-dimensional (1D) and quasi-1D superstructures formed on semiconductor surfaces by the adsorption of metal atoms have been subject of much interest due to their fundamental and technological importance. From a scientific point of view, various exotic physical phenomena such as formations of non-Fermi-liquid-like ground states, Peierls-like phase transitions, or order-disorder transitions¹⁻⁶ have been reported for these 1D structures. These observations led to a profound interest to measure the electronic structure of the Ca/Si(111) surface, which is known to form a series of quasi-1D ($n \times 2$) reconstructions ($n=3, 5, 7, \text{ and } 9$) that culminates with a 1D (2×1) phase at 0.5 monolayer (ML).⁷⁻⁹

The lowest coverage (3×2) phase, with a Ca coverage of 1/6 ML, has been proposed to be ordered according to the honeycomb-chain-channel (HCC) structure¹⁰⁻¹² while the Seiwatz structure (Ref. 13) has been proposed for the highest coverage (2×1) phase.⁷⁻⁹ The intermediate phases [the (5×2), (7×2), and (9×2) phases] are considered as combinations of the HCC and Seiwatz structures.⁷⁻⁹ The experimental surface band structure of the (3×2) phase was reported to be semiconducting,^{14,15} and shows good agreement with the calculated band structure of the Li/Si(111)-(3×1) surface that was obtained using the HCC model (Ref. 10). The good agreement between the experimental and calculated surface band structures supports the HCC model for the basic structure of the Ca induced (3×2) phase. Further, the (3×2) surface with a 1/6 ML Ca coverage, and the (3×1) surface with a 1/3 ML Li coverage, are similar in the sense that they have the same number of valence electrons per (3×1) cell. This indicates that the interaction between the Ca and Si atoms is rather ionic, which supports the proposal¹⁶ that a donation, from the metal to the silicon, of one electron per (3×1) cell is necessary in order to stabilize the HCC reconstruction of the Si substrate.

Regarding the other Ca/Si(111) phases, although all of them were reported to show semiconducting electronic structures,⁷ there is no detailed experimental study of their surface band structures so far. The structures of the interme-

mediate phases are proposed to be a combination of the (3×2) and (2×1) phases and it is therefore essential to first understand the surface band structures of these end phases. Since the surface electronic structure of the (3×2) phase is already comprehended, it means that the determination of the surface band structure of the (2×1) phase is quite important to fully understand the electronic properties of the Ca induced 1D and quasi-1D reconstructions on a Si(111) surface. Moreover, no strong evidence has been reported regarding the atomic structure of the (2×1) phase, and the determination of the surface band structure of the (2×1) phase is thus an important input to the structure determination.

In this paper, we present detailed angle-resolved photoelectron spectroscopy (ARPES) measurements of the Ca/Si(111)-(2×1) surface. Two semiconducting surface states were observed in the bulk band gap, and one in the pocket of the bulk band projection. Qualitatively, the dispersions of the two states observed in the band gap agree well with those of the surface states obtained theoretically for a clean Si(111)-(2×1) surface with a Seiwatz structure. This indicates that the two surface states in the band gap originate from Si atoms that form a Seiwatz chain, and therefore strongly supports the structure of the Ca/Si(111)-(2×1) surface proposed in the literature.

II. EXPERIMENTAL DETAILS

The ARPES measurements were performed at beamline 33 at the MAX-I synchrotron radiation facility in Lund, Sweden. Photoemission spectra were obtained using an angle-resolved photoelectron spectrometer and linearly polarized synchrotron radiation light using three different photon energies ($h\nu=17, 21.2, \text{ and } 35 \text{ eV}$). The total experimental energy resolutions were $\sim 45 \text{ meV}$ at $h\nu=17 \text{ eV}$, $\sim 50 \text{ meV}$ at $h\nu=21.2 \text{ eV}$, and $\sim 100 \text{ meV}$ at $h\nu=35 \text{ eV}$, and the angular resolution was $\pm 2^\circ$. A Si(111) sample (n type) with a 1.1° miscut towards the $[\bar{1}\bar{1}2]$ direction was cleaned by direct resistive heating following the procedure described in Refs. 17 and 18. After the cleaning, a sharp (7×7) low-energy electron diffraction (LEED) pattern was observed, and neither the valence-band spectra nor the Si $2p$ core-level

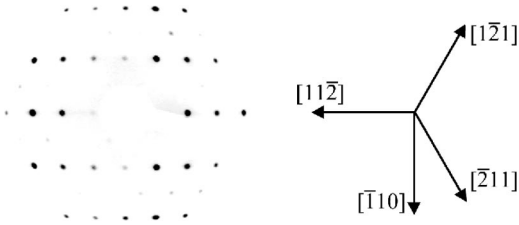


FIG. 1. LEED pattern of the Ca/Si(111)-(2 \times 1) surface obtained with a primary electron energy of 124 eV.

spectra showed any indication of contamination. Ca was evaporated from a thoroughly outgassed Knudsen cell-type evaporator onto the clean Si surface at a substrate temperature of ~ 850 K. The base pressure was below 4×10^{-11} Torr during the measurements, and below 5×10^{-10} Torr during the Ca evaporation.

Figure 1 shows the LEED pattern of the Ca/Si(111)-(2 \times 1) surface obtained after the Ca evaporation. Strong $\times 2$ spots are observed in the $[11\bar{2}]$ direction, whereas only quite weak $\times 2$ spots are observed in the $[1\bar{2}1]$ and $[\bar{2}11]$ directions. This indicates that a single-domain Ca/Si(111)-(2 \times 1) surface of quite high quality was obtained, and thus ARPES spectra can be analyzed without the ambiguity caused by contributions from the two other (2 \times 1) domains in the spectra.

III. RESULTS AND DISCUSSION

In Fig. 2, we show (a) the ARPES spectra of the Ca/Si(111)-(2 \times 1) surface measured along the $[\bar{1}10]$ and $[11\bar{2}]$ directions using $h\nu=21.2$ eV and 17 eV, together with (b) the Surface Brillouin zones (SBZ's) of the Si(111)-(1 \times 1) and (2 \times 1) surfaces. The spectra in the $[11\bar{2}]$ direction were measured using the in-plane polarization geometry (the electric field of photons is parallel to the photoelectron emission plane) and the spectra in the $[\bar{1}10]$ direction were obtained using the out-of-plane polarization geometry (the photoelectron emission plane is perpendicular to that of the in-plane polarization geometry). As indicated in Fig. 2(b), the $[\bar{1}10]$ direction corresponds to the $\bar{\Gamma}-\bar{J}-\bar{K}-\bar{\Gamma}(\bar{M})$ direction, and the $[11\bar{2}]$ direction corresponds to the $\bar{\Gamma}-\bar{J}'-\bar{\Gamma}(\bar{M})$ direction. The symbols \bar{M} and \bar{K} are the symmetry points of the (1 \times 1) SBZ, and the symbols \bar{J} and \bar{J}' are the symmetry points of the (2 \times 1) SBZ. The angle-resolved photoelectron spectra were recorded at every 1° from emission angles (θ_e) of -2° to 61° in the $[\bar{1}10]$ direction, and at every 1° from $\theta_e=0^\circ$ to 34° in the $[11\bar{2}]$ direction. The Fermi-level position (E_F) that is indicated by dashed lines, was determined by measuring the metallic Fermi edge of a Ta foil fixed on the sample holder. Compared to the spectra observed using $h\nu=21.2$ eV, the cross section of the state with a binding energy of approximately 1 eV is larger using $h\nu=17$ eV at small θ_e . The binding energy of this state becomes larger as θ_e increases in the $[\bar{1}10]$ direction, and becomes smaller in the $[11\bar{2}]$ direction. Since this state does not cross the Fermi

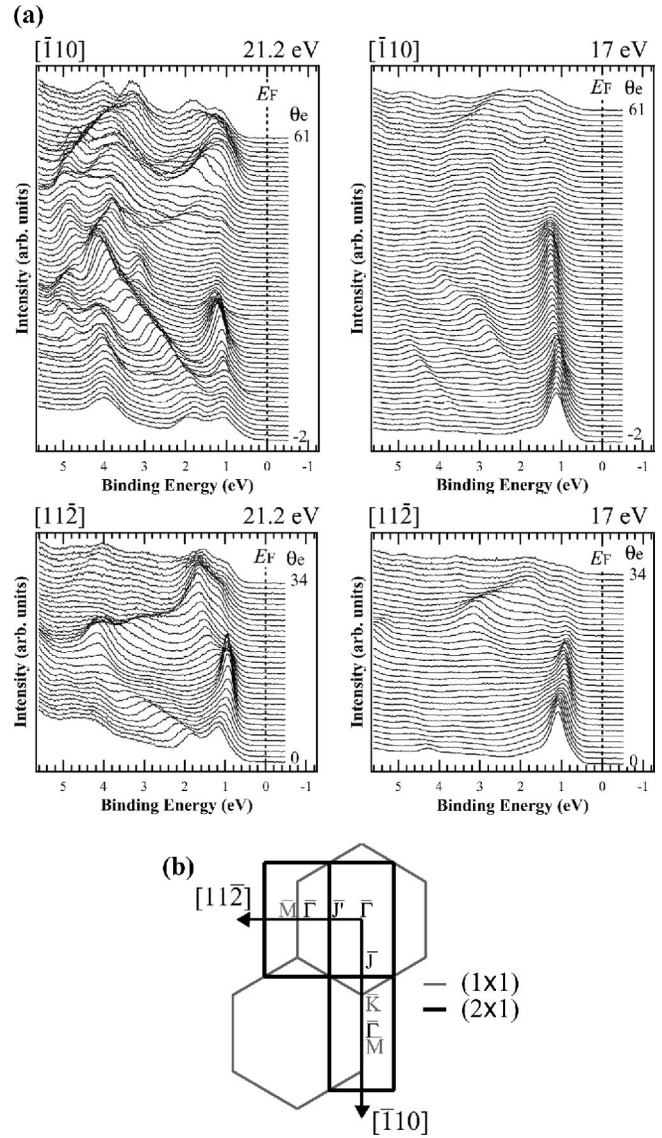


FIG. 2. (a) ARPES spectra of the Ca/Si(111)-(2 \times 1) surface measured along the $[\bar{1}10]$ and $[11\bar{2}]$ directions using $h\nu=21.2$ and 17 eV. The spectra in the $[\bar{1}10]$ and $[11\bar{2}]$ directions were measured using the out-of-plane polarization geometry and the in-plane polarization geometry, respectively. The angle-resolved photoelectron spectra were recorded at every 1° in both directions. (b) Surface Brillouin zones of the Si(111)-(1 \times 1) and (2 \times 1) surfaces. Black letters are the symmetry points of the (2 \times 1) SBZ and the gray letters are those of the (1 \times 1) SBZ.

level and no other state is observed at lower binding energies, we conclude that the electronic structure of the Ca/Si(111)-(2 \times 1) surface is semiconducting. This agrees well with the result of the angle-integrated valence band study⁷ in which no density of states was observed at the Fermi level.

Figure 3 displays the band dispersions of the Ca/Si(111)-(2 \times 1) surface along the $[\bar{1}10]$ and $[11\bar{2}]$ directions obtained using $h\nu=21.2$ eV and 17 eV. The bold dashed lines are the valence-band edge and edges of pockets taken from Ref. 19, and the thin dashed lines represent the symmetry points of the (1 \times 1) and (2 \times 1) SBZ's indicated at the top

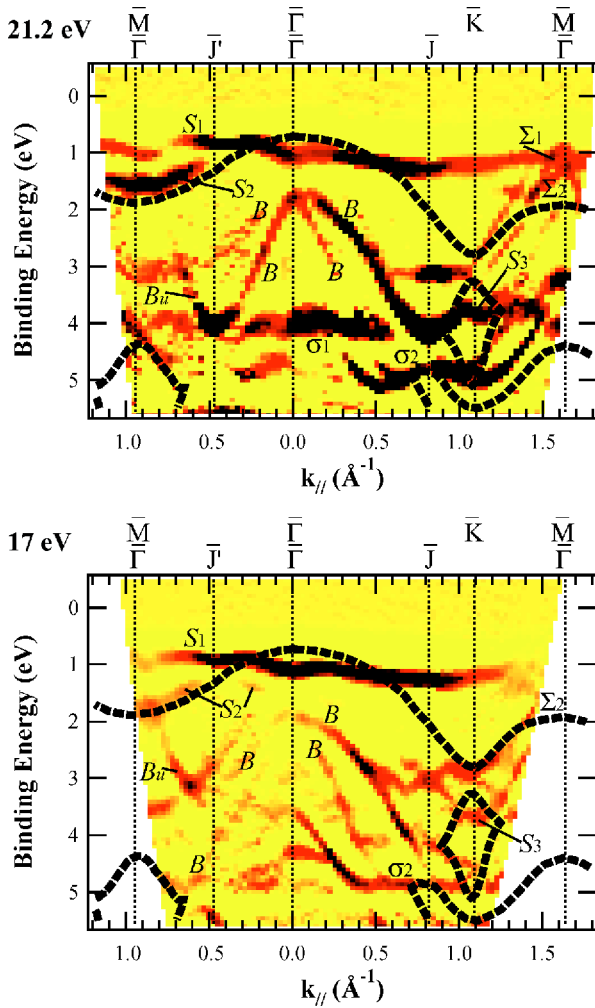


FIG. 3. (Color online) Band dispersion of the Ca/Si(111)-(2×1) surface measured along the $[11\bar{2}]$ and $[\bar{1}10]$ directions using $h\nu=21.2$ eV and $h\nu=17$ eV. The bold dashed lines are the valence-band edge and edges of pockets taken from Ref. 19, and the thin dashed lines represent the symmetry points indicated at the top of each figure.

of each figure. The valence-band maximum (VBM) is estimated from the binding energy of the Si $2p$ core level using the relation between $E_{B(\text{VBM})}$, E_F , and $E_{B(\text{Si}2p_{3/2})}$ given in Ref. 20. The intensities of the spectral features are approximately represented by the brightness of the grayscale which represents the second derivatives of the original ARPES spectra. Here we note that the validity of the use of the second derivative of the spectra has been confirmed by comparing the binding energies and brightness from Fig. 3 with binding energies and intensities of the spectral features in Fig. 2.

Three surface states, labeled $S_1 - S_3$, are clearly observed in the band gap and pockets of the bulk band projection in Fig. 3. S_1 , which is the surface state observed as a prominent peak in the spectra using $h\nu=17$ eV in Fig. 2, disperses first slightly upward and then downward between the $\bar{\Gamma}$ and \bar{J} points. In the second SBZ, the dispersion is upward from the \bar{J} point to the $\bar{\Gamma}$ point. Between the $\bar{\Gamma}$ point and the \bar{J} point

the S_1 band shows an upward dispersion and a downward dispersion between the \bar{J}' point and the $\bar{\Gamma}$ point of the second SBZ. The dispersion width of the S_1 state is approximately 0.15 eV in the $[\bar{1}10]$ direction, and it is approximately 0.25 eV in the $[11\bar{2}]$ direction. The S_2 state is only observed in the $[11\bar{2}]$ direction, and disperses downward from the \bar{J}' point to the $\bar{\Gamma}$ point of the second SBZ using $h\nu=21.2$ and 17 eV. This S_2 state is also observed faintly between the $\bar{\Gamma}$ point to the \bar{J}' point using $h\nu=17$ eV. The dispersion features of the S_1 and S_2 states indicate that these two surface states follow a (2×1) periodicity. Concerning S_3 , we cannot give its dispersion features since this state is only observed in a small $k_{||}$ region.

In addition to the three surface states, five other states (the B_u , Σ_1 , Σ_2 , σ_1 , and σ_2 states), which are not observed on the Si(111)-(7×7) surface, are shown in Fig. 3. Three origins can be considered for these five states. That is, direct bulk transitions, folding of bulk states by umklapp processes, and surface states or resonance states. The B_u state, which completely follows the (2×1) periodicity, has the same dispersion features in both the $[11\bar{2}]$ and $[\bar{1}\bar{1}2]$ directions (the dispersion in the $[\bar{1}\bar{1}2]$ direction is not shown in this paper), should not originate from bulk transitions since such bulk features show different dispersions in the $[11\bar{2}]$ and $[\bar{1}\bar{1}2]$ directions (Ref. 21). Further, taking into account that the dispersion of B_u from the \bar{M} point to the \bar{J}' point is quite similar to that of the B state from the $\bar{\Gamma}$ point to the \bar{J}' point, we conclude that the B_u state results from the folding of B by a reciprocal lattice vector of the high quality (2×1) surface used in the present study. Regarding the Σ_1 and Σ_2 states, which are observed in the bulk band gap, they disperse upward from the \bar{K} point to the \bar{M} point. The calculated binding energies of bulk transitions are much higher than those of Σ_1 and Σ_2 at the \bar{M} point.²¹ Moreover, no structures that could be the origins of Σ_1 and Σ_2 are observed around the $\bar{\Gamma}$ point. Thus, Σ_1 and Σ_2 might be surface states. The σ_1 state is observed clearly around the $\bar{\Gamma}$ point of the (1×1) SBZ using $h\nu=21.2$ eV, and has almost no dispersion. σ_2 , whose binding energy is approximately 4.8 eV at the \bar{K} point, has an upward dispersion from the \bar{K} point to the \bar{M} point. Since this is roughly the dispersion expected for a direct transition at $h\nu=21.2$ eV,²¹ the origin of σ_2 might be a direct bulk transition. However, we do not discuss the B_u , Σ_1 , Σ_2 , σ_1 , and σ_2 states more due to the lack of detailed information.

In order to discuss the surface electronic structure of the Ca/Si(111)-(2×1) surface in more detail, we compare the band dispersions of the two surface states observed in the bulk band gap (the S_1 and S_2 states) with the dispersions of the surface states obtained by the theoretical calculations performed for the Si(111)-(2×1) clean surface with Seiwatz structure.^{22,23} Here we note that although the structure of the Si(111)-(2×1) surface is called the three-bond scission (TBS) model in Refs. 22 and 23, we use the name Seiwatz in the present paper since first the structures of the two models

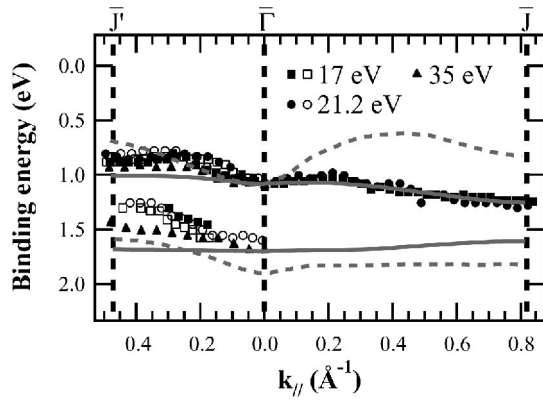


FIG. 4. Surface-state dispersions of the Ca/Si(111)-(2 \times 1) surface along the \bar{J}' - $\bar{\Gamma}$ - \bar{J} symmetry lines. The filled squares, circles, and triangles represent the peak and shoulder positions of the ARPES spectra obtained using $h\nu=17$, 21.2, and 35 eV, respectively. The open squares and circles are those obtained in the \bar{J}' - Γ_{2nd}^- direction (Γ_{2nd}^- means the $\bar{\Gamma}$ point of the second Brillouin zone) with $h\nu=17$ and 21.2 eV. Solid (Ref. 22) and dashed (Ref. 23) gray lines are the theoretical surface-state dispersions derived from calculation for the Si(111)-(2 \times 1) clean surface with Seiwatz structures.

are basically the same, and second the name Seiwatz was used in the literature on the Ca/Si(111)-(2 \times 1) surface. Further, since the interaction between Ca and Si atoms would be ionic on a Ca/Si(111)-(2 \times 1) surface likewise the interaction on a Ca/Si(111)-(3 \times 2) surface, we compare the S_1 and S_2 states with the two surface states of the Si(111)-(2 \times 1) clean surface that are originally situated just above and just below the Fermi level. The filled squares and circles in Fig. 4 represent the peak and shoulder positions of the ARPES spectra obtained along \bar{J}' - $\bar{\Gamma}$ - \bar{J} using $h\nu=17$ and 21.2 eV, respectively, and the filled triangles represent those obtained along the $\bar{\Gamma}$ - \bar{J}' direction using $h\nu=35$ eV (spectra are not shown in this paper). The open squares and circles are the peak and shoulder positions of the ARPES spectra obtained along the \bar{J}' point to the $\bar{\Gamma}$ point of the second Brillouin zone using $h\nu=17$ and 21.2 eV, and plotted in the $\bar{\Gamma}$ - \bar{J} direction by considering the symmetry of the surface-state band structure. The gray solid lines are the dispersions of the surface states derived from the theoretical calculations in Ref. 22, and the gray dashed lines are those derived from Ref. 23. The binding energies of the calculated surface states are shifted to fit the upper calculated surface states to the binding energy of the S_1 state at the $\bar{\Gamma}$ point. Concerning the gray solid lines, the dispersion widths of the two calculated surface states and the gap between them were reduced by a factor of 10 from their original values (the factor was chosen to fit the calculated gap and the gap between S_1 and S_2) by considering that the dispersion widths and the band gap reported in Ref. 22 were stated to be overestimated.²³

As shown in Fig. 4, although the two calculations were performed using different methods (the Hartree-Fock approximation method was used in Ref. 22 and the local-density approximation method in Ref. 23) and different magnitude of buckling for Si atoms forming Seiwatz chains, the

dispersion behaviors of the two surface states are similar. That is, the upper surface state disperses first slightly upward and then downward from the $\bar{\Gamma}$ point to the \bar{J} point and upward from the $\bar{\Gamma}$ point to the \bar{J}' point, and the lower surface state disperses upward in both the $\bar{\Gamma}$ - \bar{J} and the $\bar{\Gamma}$ - \bar{J}' directions (it is hard to observe the upward dispersions of the gray solid lines in Fig. 4 but they are clear in Ref. 22). These dispersion behaviors agree well with those of S_1 and S_2 . Compared with the dispersions of the surface states of the Si(111)-(2 \times 1) clean surface with the Seiwatz structure, those of the Si(111)-(2 \times 1) clean surface with other structures, i.e., the Pandey π -bonded chain structure,²⁴ the Chadi π -bonded molecular structure,²⁵ and the buckling structure,²⁶ are different. The corresponding two surface states disperse downward in the $\bar{\Gamma}$ - \bar{J}' direction with a Pandey π -bonded chain structure,^{23,27} the lower surface state has a downward dispersion in the $\bar{\Gamma}$ - \bar{J}' direction with a Chadi π -bonded molecular structure,²⁸ and the upper surface state has only a continuative downward dispersion in the $\bar{\Gamma}$ - \bar{J} direction with a buckling structure.^{22,28,29} This indicates that only the dispersion behaviors of the surface states of a clean surface with a Seiwatz structure agree with those of the S_1 and S_2 states. Taking into account that an ionic interaction hardly affects the dispersion behaviors of surface states and that a difference in magnitude of buckling might cause different dispersion widths, we conclude that the S_1 and S_2 states originate from orbitals of Si atoms that form a Seiwatz structure. Moreover, the observation of the semiconducting S_1 state suggests that the lowest unoccupied surface state of the Si(111)-(2 \times 1) clean surface with a Seiwatz structure is fully occupied by the donation of two electrons per (2 \times 1) unit cell. The presence of a Seiwatz structure and the number of electrons per unit cell, which corresponds to a 0.5 ML Ca coverage, strongly support the surface structure of the Ca/Si(111)-(2 \times 1) surface proposed in the literature.⁷⁻⁹

IV. CONCLUSION

In conclusion, we have studied the electronic structure of the Ca/Si(111)-(2 \times 1) surface by ARPES using different photon energies. Two semiconducting surface states (S_1 and S_2) were clearly observed in the bulk band gap, and one (S_3) in a pocket of the bulk band projection. The dispersions of S_1 and S_2 completely follow a (2 \times 1) periodicity. The S_1 state disperses slightly upward and then downward from the $\bar{\Gamma}$ point to the \bar{J} point, and upward from the $\bar{\Gamma}$ point to the \bar{J}' point, and the S_2 state, which is only observed in the $[\bar{1}\bar{1}\bar{2}]$ direction has an upward dispersion from the $\bar{\Gamma}$ point to the \bar{J}' point. These dispersion features agree well with the dispersions of the surface states obtained theoretically for a clean Si(111)-(2 \times 1) surface with a Seiwatz structure. Taking the ionic interaction between Ca and Si atoms into account, we conclude that the S_1 and S_2 states originate from orbitals of Si atoms that form a Seiwatz structure. This is a strong evidence that the Ca/Si(111)-(2 \times 1) surface is formed by a Seiwatz structure with a 0.5 ML Ca coverage as proposed in the literature.

ACKNOWLEDGMENTS

Experimental support from Dr. T. Balasubramanian and the MAX-lab staff, and suggestions on the sample prepara-

tion from Dr. T. Sekiguchi are gratefully acknowledged. This work was financially supported by the Swedish Research Council and the Ministry of Education, Culture, Sports, Science and Technology of the Japanese Government.

*Electronic address: sakamoto@surface.phys.tohoku.ac.jp

- ¹P. Segovia, D. Purdie, M. Hengsberger, and Y. Baer, *Nature* (London) **402**, 504 (1999).
- ²H.W. Yeom, S. Takeda, E. Rotenberg, I. Matsuda, K. Horikoshi, J. Schaefer, C.M. Lee, S.D. Kevan, T. Ohta, T. Nagao, and S. Hasegawa, *Phys. Rev. Lett.* **82**, 4898 (1999).
- ³O. Gallus, Th. Pillo, M. Hengsberger, P. Segovia, and Y. Baer, *Eur. Phys. J. B* **20**, 313 (2001).
- ⁴R. Losio, K.N. Altmann, A. Kirakosian, J.L. Lin, D.Y. Petrovykh, and F.J. Himpsel, *Phys. Rev. Lett.* **86**, 4632 (2001).
- ⁵I.K. Robinson, P.A. Bennett, and F.J. Himpsel, *Phys. Rev. Lett.* **88**, 096104 (2002).
- ⁶K. Sakamoto, H. Ashima, H.M. Zhang, and R.I.G. Uhrberg, *Phys. Rev. B* **65**, 045305 (2002).
- ⁷A.A. Baski, S.C. Erwin, M.S. Turner, K.M. Jones, J.W. Dickinson, and J.A. Carlisle, *Surf. Sci.* **476**, 22 (2001).
- ⁸T. Sekiguchi, F. Shimokoshi, T. Nagao, and S. Hasegawa, *Surf. Sci.* **493**, 148 (2001).
- ⁹K. Sakamoto, W. Takeyama, H.M. Zhang, and R.I.G. Uhrberg, *Phys. Rev. B* **66**, 165319 (2002).
- ¹⁰S.C. Erwin and H.H. Weitering, *Phys. Rev. Lett.* **81**, 2296 (1998).
- ¹¹L. Lottermoser, E. Landemark, D.-M. Smilgies, M. Nielsen, R. Feidenhans'l, G. Falkenberg, R.L. Johnson, M. Gierer, A.P. Seitsonen, H. Kleine, H. Bludau, H. Over, S.K. Kim, and F. Jona, *Phys. Rev. Lett.* **80**, 3980 (1998).
- ¹²M.-H. Kang, J.-H. Kang, and S. Jeong, *Phys. Rev. B* **58**, R13 359 (1998).
- ¹³R. Seiwatz, *Surf. Sci.* **2**, 473 (1964).
- ¹⁴D.Y. Petrovykh, K.N. Altmann, J.-L. Lin, F.J. Himpsel, and F.M. Leibsle, *Surf. Sci.* **512**, 269 (2002).
- ¹⁵O. Gallus, Th. Pillo, P. Starowicz, and Y. Baer, *Europhys. Lett.* **60**, 903 (2002).
- ¹⁶G. Lee, S. Hong, H. Kim, D. Shin, J.-Y. Koo, H.-I. Lee, and D.W. Moon, *Phys. Rev. Lett.* **87**, 056104 (2001).
- ¹⁷J. Viernow, J.-L. Lin, D.Y. Petrovykh, F.M. Leibsle, F.K. Men, and F.J. Himpsel, *Appl. Phys. Lett.* **72**, 948 (1998).
- ¹⁸J.-L. Lin, D.Y. Petrovykh, J. Viernow, F.K. Men, D.J. Seo, and F.J. Himpsel, *J. Appl. Phys.* **84**, 255 (1998).
- ¹⁹J. Ihm, M.L. Cohen, and J.R. Chelikowsky, *Phys. Rev. B* **22**, 4610 (1980).
- ²⁰F.J. Himpsel, G. Hollinger, and R.A. Pollak, *Phys. Rev. B* **28**, 7014 (1983).
- ²¹R.I.G. Uhrberg, G.V. Hansson, J.M. Nicholls, P.E.S. Persson, and S.A. Flodström, *Phys. Rev. B* **31**, 3805 (1985), and references therein.
- ²²B. Chen and D. Haneman, *Phys. Rev. B* **51**, 4258 (1995).
- ²³S.-H. Lee and M.-H. Kang, *Phys. Rev. B* **54**, 1482 (1996).
- ²⁴K.C. Pandey, *Phys. Rev. Lett.* **47**, 1913 (1981).
- ²⁵D.J. Chadi, *Phys. Rev. B* **26**, 4762 (1982).
- ²⁶D. Haneman, *Phys. Rev.* **121**, 1093 (1961).
- ²⁷J.E. Northrup and M.L. Cohen, *Phys. Rev. Lett.* **49**, 1349 (1982).
- ²⁸D. Vanderbilt and S.G. Louie, *J. Vac. Sci. Technol. B* **1**(3), 723 (1983).
- ²⁹R. Del Sole and D.J. Chadi, *Phys. Rev. B* **24**, 7431 (1981).